

# OXIDATION RESISTANCE AND MICROSTRUCTURE OF Pt AND PtIr DIFFUSION COATINGS ON Ni BASED SINGLE CRYSTAL SUPERALLOYS BY ELECTROPLATING METHOD

Dao Chi Tue<sup>1,2,\*</sup>, Hideyuki Murakami<sup>2,3</sup>, Le Thi Hong Lien<sup>1</sup>

<sup>1</sup>Center of Failure Analysis, Institute of Materials Science, 18 Hoang Quoc Viet, Cau Giay, Ha Noi, Viet Nam

<sup>2</sup>Research Center for Structural Materials, National Institute for Materials Science, Sengen 1-2-1, Tsukuba, Ibaraki, 305-0047, Japan

<sup>3</sup>Department of Nanoscience and Nanoengineering, Graduate School of Advanced Science and Engineering, Waseda University, 3-4-1, Okubo, Shinjuku-ku, 169-8555, Japan

\*Email: [tuedc@ims.vast.vn](mailto:tuedc@ims.vast.vn)

Received: 30 April 2019; Accepted for publication: 26 August 2019

**Abstract:** Blades and vanes for gas turbines, usually made of Ni-based superalloys, are exposed at very high temperature in severe oxidation and corrosion environments. Nowadays, thermal barrier coating systems (TBCs) have been applied to protect them against such severe working conditions. In this study, Pt and PtIr diffusion coatings on Ni based single crystal superalloys were fabricated by an electroplating method followed by an annealing heat treatment process. The microstructure and phase constitution of the coatings were studied by SEM/EDS and XRD methods. The cyclic oxidation test at 1150 °C was conducted to investigate the oxidation resistance of the coatings. The results showed that the addition of Ir in the coating led to the formation of  $\alpha$ (NiPt<sub>2</sub>Al) phase and reduced the formation of Kirkendall voids in the coating after 100 cycle oxidation test.

**Keywords:** Platinum-Iridium, diffusion coating, electroplating, microstructure change, gas turbine.

**Classification numbers:** 2.5.3; 2.9.1.

## 1. INTRODUCTION

Ni-based single crystal superalloys generally possess superior high temperature mechanical strength and creep resistance, thus they have been used in the hottest section of gas turbines such as blades. To protect Ni-based alloys against high temperature oxidation and corrosion, thermal barrier coating (TBC) systems were applied [1, 2]. Basically, TBCs consist of a ceramic top coat (TC) that provides thermal insulation, metallic bond coat (BC) and a thermally grown oxide (TGO) which bonds TC and BC. Among them, the BC not only supports the bonding of the TC to substrate material but also works as an Al reservoir to form TGO layer during exposure at high temperature of TBCs. The TGO, which mainly consists of an  $\alpha$ -alumina, prevents further oxidation of BC and substrate alloy, thus the BC should have Al-enriched layer on the top.

There are several types of bond-coats, such as Pt-modified aluminide coatings and MCrAlY overlay coatings. They both have high concentration of aluminum with  $\beta$ -AlNi-type phase microstructure. However,  $\beta$ -containing coatings suffer from transformation from  $\beta$  to  $\gamma'$ -Ni<sub>3</sub>Al or  $\gamma$ -Ni solid solution phase, which leads to surface rumpling, and interdiffusion between substrates and coatings leads to the formation of intermetallic phases with brittle topologically close-packed (TCP) structure in service, which results in the degradation of coated materials [3]. To overcome such problems, recently, Pt diffusion coatings with the  $\gamma+\gamma'$  phase microstructure, similar with that of substrate, have been proposed and their oxidation resistance have been reported [4-6]. It has been shown that they could reduce the rumpling [5, 7, 8] and limit or suppress the precipitation of brittle TCP phases [7].

In order to further increase efficiency and reducing CO<sub>2</sub> emission of gas turbines, there is a continuous requirement to develop a better coating which stands for higher temperature environments. Pt diffusion coating is expected to be modified by the addition of platinum group metal (PGM) elements. Indeed, palladium [9], rhodium or iridium [10] addition has been attempted. Among PGMs, iridium is interested since it has the highest melting temperature (2716 K), high tensile strength (440 MPa) at room temperature, excellent chemical stability, and lower diffusivity into Ni-base alloys than Pt [11]. It is expected that the addition of Ir into Pt diffusion coating may improve the oxidation resistance and prolong life time of coated materials. There are some studies of the authors' group showing that Ir addition improved high temperature oxidation resistance of the Pt-modified aluminide coatings [12-14]. However, research about effects of Ir addition to Pt-diffusion coatings on microstructure and oxidation resistance of Ni-based single crystal superalloys needs further investigation.

In this study, the Pt and Pt20 at %Ir diffusion bond-coatings, developed by the electroplating method on the Ni-based single crystal superalloy UCSX-8 was investigated. The phase transformation and the microstructure change of the coating during cyclic oxidation tests were analyzed to understand the effect of Ir addition to the oxidation resistance of the coating.

## 2. MATERIALS AND METHODS

A so-called 4<sup>th</sup> generation Ni-based single crystal superalloy UCSX-8 was used as a substrate material. Its nominal composition is Ni (bal.)-6.4 Co-1.8 Cr-3.6 Mo-4.1 W-5.2 Re-2.1 Ru-6.8 Al-10.0 Ta (mass %). The substrate material, single-crystal bar 10 mm in diameter, was solution heat treated at 1355 °C for 20 hours to form  $\gamma+\gamma'$  structure and then was cut into discs 2 mm in thickness, mechanically polished with SiC paper up to #800 and degreased with acetone for 5 minutes in an ultrasonic bath. The Pt and PtIr films were deposited on the surface of the specimen by an electroplating method. The Pt film of 8  $\mu$ m thickness was electroplated on the surface of specimens. For the Pt20Ir (at%) film, to enhance the bonding of coating to substrate, a 2  $\mu$ m of Pt film was electroplated on the surface as a bonding layer. Then, a 6  $\mu$ m of Pt20Ir film was electroplated subsequently on the Pt layer. The electroplating solution and process parameters are showed in Table 1 and Table 2. All above specimens were diffusion heat treated for 1 hour at 1100 °C in an Ar flow with a pressure of 0.3 MPa to protect coatings from oxidation.

The cyclic oxidation test at 1150 °C in still air was carried out to investigate the change of coating microstructure. All the specimens were tested up to 100 cycles. The sample surface, cross-sectional morphologies and element concentration profiles along the cross-section of the coatings were analyzed by a field-emission scanning electron microscope (FE-SEM, Hitachi S4700) equipped with an X-ray energy dispersive spectrometer (EDS). The working distance

(WD) around 10 mm was used for EDS analysis. The crystal structure of the coatings was identified by X-ray diffractometer using RINT-2500/PC equipment (radiation  $\text{CuK}\alpha$ , 40 kV/300 mA).

Table 1. Pt electroplating conditions.

$\text{K}_2\text{Pt}(\text{OH})_6$	Pt 15 g/l
KOH	10-15 g/l
$\text{CH}_3\text{COONa}$	50 g/L
Citric acid $\text{C}_6\text{H}_7\text{O}_6$	3 g/l
pH	13.19
Temperature	93-94 °C
Current density	1 A/dm <sup>2</sup>
Plating time	1 hr.
Rotation	400 rpm
Electrode	Pt/Ti

Table 2. PtIr electroplating conditions.

$\text{Na}_3\text{IrB}_6$	Ir 5 g/l
$\text{K}_2\text{PtCl}_4$	Pt 2 g/l
NaBr	1 M/l
NaCl	0.5 M/l
$\text{C}_{10}\text{H}_{14}\text{N}_2\text{Na}_2\text{O}_8 \cdot 2\text{H}_2\text{O}$	2 g/l
Citric acid $\text{C}_6\text{H}_8\text{O}_7$	2 g/l
pH	1.16
Temperature	85 °C
Current density	1 A/dm <sup>2</sup>
Plating time	30 min.
Rotation	600 rpm
Electrode	Pt/Ti

### 3. RESULTS AND DISCUSSIONS

The addition of Ir into Pt electroplating affects the microstructure of the coating layer. The surface of Pt electroplated specimen shows dense, uniform structure without any cracking (Fig.1a). When Ir was added to the coating, high residual stress of electroplated alloys and the formation of  $\text{H}_2$  gas in the electroplating process lead to the cracking on the surface of as-deposited specimens (Fig.1b). The surface appearance of Pt20Ir coating looks grey, less bright than that of Pt coating. After the heat treatment, the cracking of the coating surface seems a little reduced by the sintering effect and the interdiffusion of elements between the coating layer and the substrates.

Figure 2 shows the cross-sectional microstructure and elements distribution in the coating layers of Pt and Pt20Ir after annealing heat treatment. By the back-scatter electron (BSE) mode, the coating layers are brightly contrasted by the high concentration of Pt and Ir. The Pt electroplated coating (Fig. 2a) consisted of two layers: a Pt enriched surface layer and an interdiffusion zone (IDZ). The Pt enriched layer with the thickness of approximately 8  $\mu\text{m}$  is the original electroplated coating containing the outwardly diffusing elements from the substrate. The IDZ, about 24  $\mu\text{m}$  in thickness is formed by the annealing process, mainly due to the inward diffusion of Pt from the coating layer to the substrate. The microstructure of Pt20Ir coating having three layers is shown in Fig. 2b. It consists of a 6  $\mu\text{m}$  Pt-Ir enriched surface layer, a 2  $\mu\text{m}$  Pt enriched layer and about 18  $\mu\text{m}$  IDZ. The elements distribution profile confirms the up-hill diffusion of Al from substrate to the surface. The Al concentration at the surface of Pt and Pt20Ir electroplated specimens are about 20 at.% and 18 at.%, respectively. For the Pt-Ir coating, most of Ir remains in the electroplated layer and apparently its inward diffusion to the IDZ is low, confirming the previous report that Ir addition in the coating lowers diffusivity of other elements in both  $\gamma$  and  $\gamma'$  structure [11]. It is thus also noted that the Pt diffusion to substrate lowered and resulted in the formation of thinner IDZ in the Pt-Ir coating than that in the Pt coating. Together

with that, Al concentration on the surface of Pt-Ir coating is also lower (about 18 at.%) than that of Pt coating (about 20 at.%). The Al concentration on the surface of coating has an important role in the formation of alumina scale which effectively protects the substrate from high temperature oxidation.

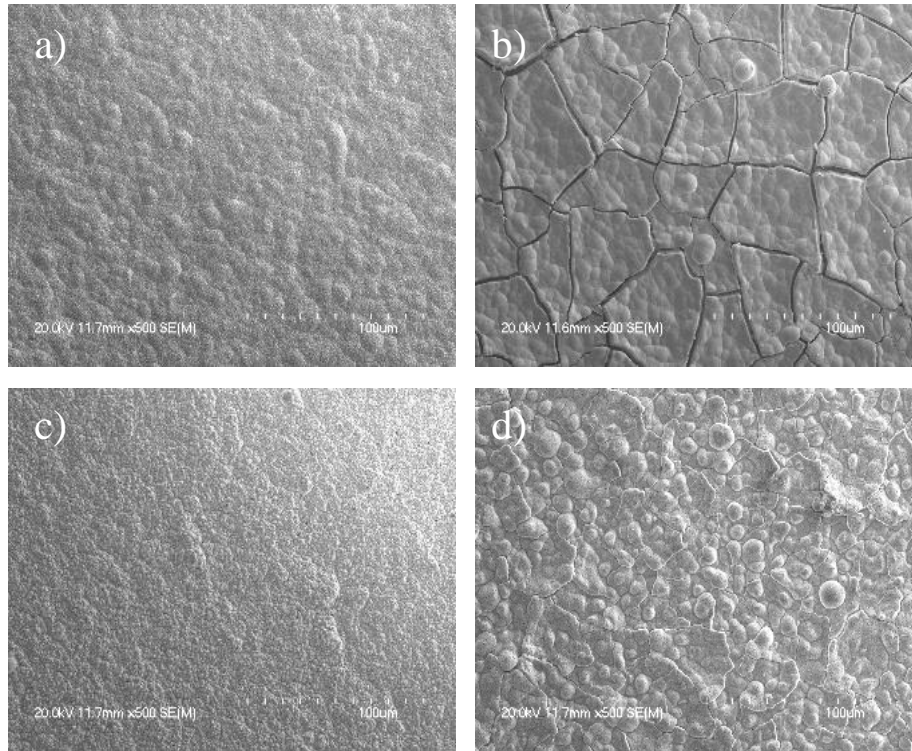


Figure 1. Surface morphologies of as electroplated and annealing specimens by SEM (SE).

- |                           |                      |
|---------------------------|----------------------|
| a) Pt as-electroplated    | c) Pt as-annealed    |
| b) PtIr as- electroplated | d) PtIr as-annealed. |

Figure 3 shows the phase constitution of the specimens' surface after the annealing heat treatment. The Pt electroplated specimen shows  $\gamma$ -Ni,Pt,Al and  $\gamma'$ -(Ni,Pt)<sub>3</sub>Al structure. The microstructure of Pt diffusion coating was investigated and confirmed by other studies [4, 15-17]. On the other hand, in the Pt20Ir electroplated coating,  $\gamma$ + $\alpha$  two phase structure was observed instead of  $\gamma$ + $\gamma'$  two phases. The  $\alpha$ -NiPtAl phase with L<sub>10</sub> crystal structure was known as Pt enriched phase and an intermediate phase in the transformation process to form  $\gamma'$  of the specific  $\gamma$ + $\gamma'$  structure of diffusion coatings [15, 18]. It is confirmed that the Ir addition affected the diffusivity of elements and resulted in the formation of an intermediate phase by the annealing treatment conducted in this study.

Figure 4 shows the change in surface appearances of samples before and after the cyclic oxidation test. After 100 cycles, the surface of Pt-diffusion specimens keeps uniform appearances without any cracks or surface spallation while in the PtIr coating, some local change in colors, probably due to the surface spallation and formation of spinel oxides, was observed.

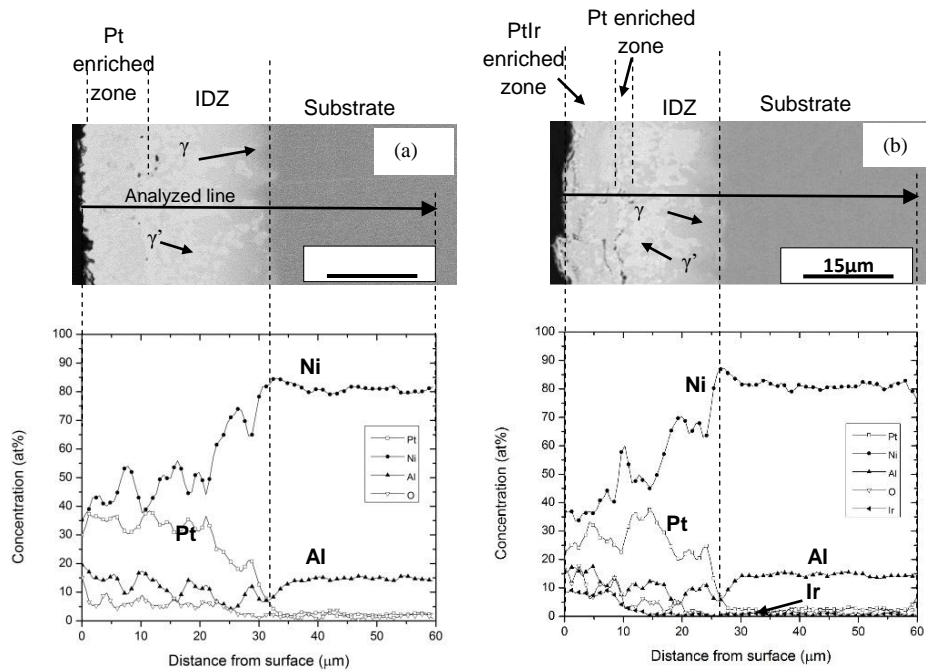


Figure 2. Cross-sectional microstructure (BSE) and corresponding elements concentration profile of as-annealed electroplated specimen: (a) Pt and (b) Pt20Ir.

More detailed surface morphology of coating could be seen in Fig. 5. The bright areas in the figure with the BSE mode evidence the enrichment of heavy elements (Pt, Ir) which remain in the coating layer. It is also confirmed from Fig. 5 that while distribution of Pt in the Pt-diffusion coating is fine and uniform, Pt and /or Ir locally concentrated in the initial stage and became less uniform after 35 cycles, compared with that of Pt-diffusion coatings.

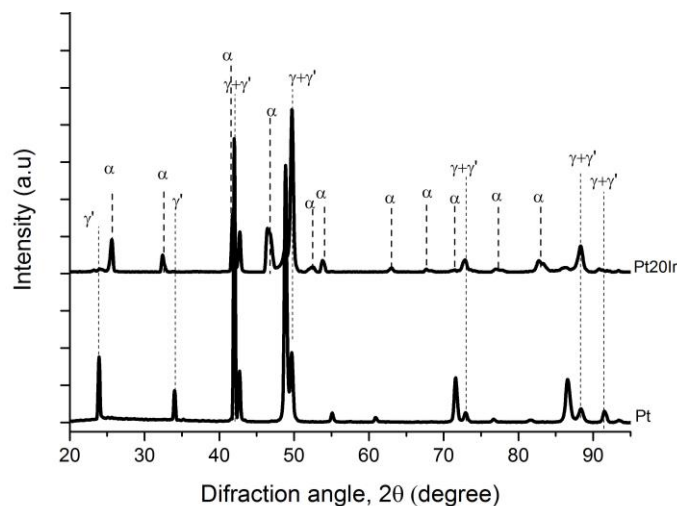


Figure 3. XRD patterns of specimens after annealing heat treatment.

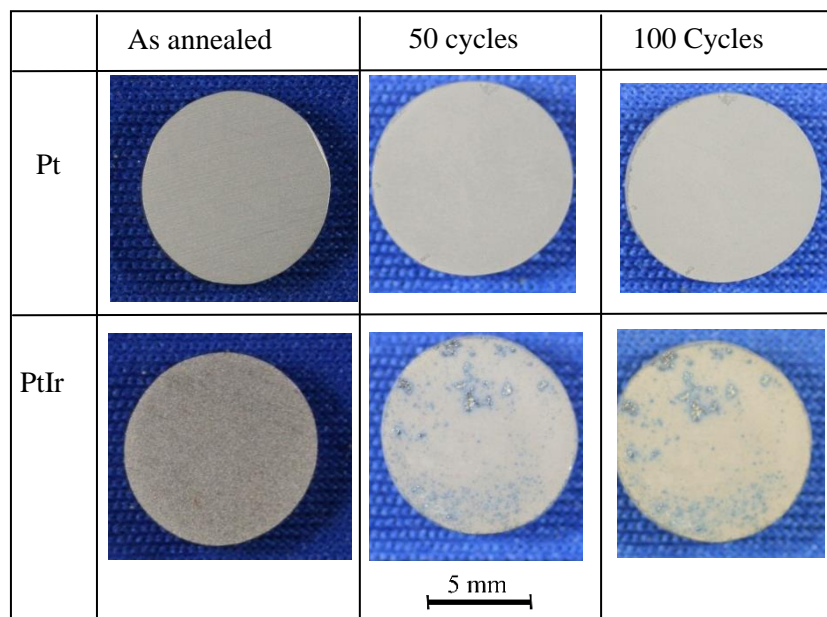


Figure 4. Surface appearance of samples before and after cyclic oxidation. test

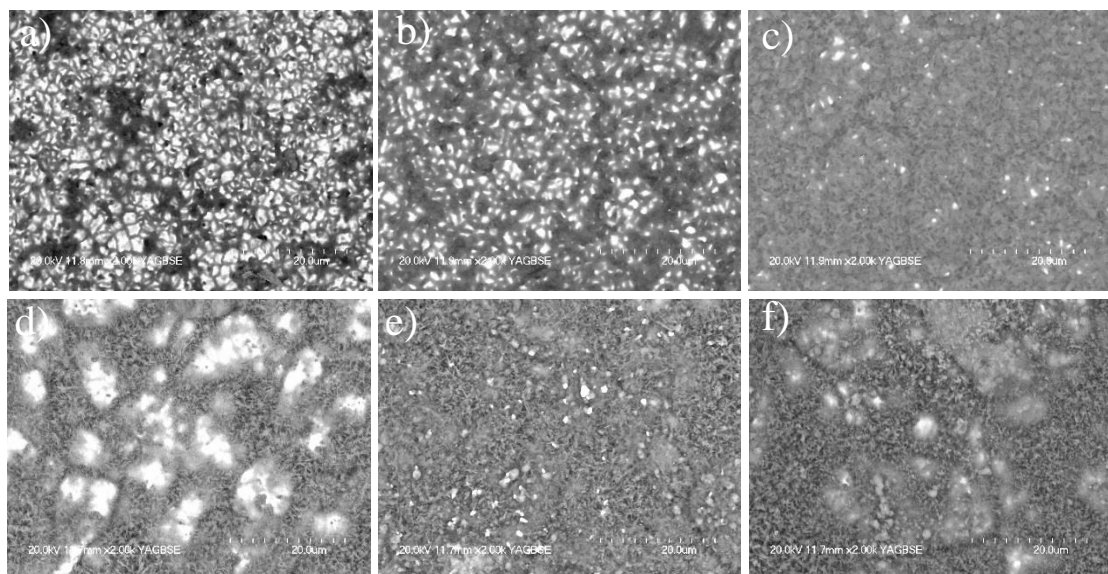


Figure 5. Surface morphology of samples after cycle tests by SEM with BSE mode

- |                           |                              |
|---------------------------|------------------------------|
| a) Pt coating, 10 cycles  | d) PtIr coating, 10 cycles   |
| b) Pt coating, 35 cycles  | e) PtIr coating, 35 cycles   |
| c) Pt coating, 100 cycles | f) PtIr coating, 100 cycles. |



Figure 6 shows the phase constitution in the specimen surface area after 100 cyclic oxidation test. The Pt-diffusion specimen showed has microstructure with diffusion structure  $\gamma+\gamma'$  in the coating layer and  $\alpha\text{-Al}_2\text{O}_3$  layer on the surface. The electroplated Pt20Ir specimen has microstructure consisting of  $\alpha\text{-Al}_2\text{O}_3$ , spinel  $\text{NiAl}_2\text{O}_4$  and  $\gamma+\gamma'$  phase. The  $\alpha\text{-NiPt}_2\text{Al}$  phase on the coating layer was completely transformed into  $\gamma'$  phase. In addition, peaks from the spinel  $\text{NiAl}_2\text{O}_4$  was observed together with  $\alpha\text{-Al}_2\text{O}_3$ . The spinel phase was formed due to the lack of Al activity to form  $\alpha\text{-Al}_2\text{O}_3$  [7]. The growth rate of spinel  $\text{NiAl}_2\text{O}_4$  is higher than that of  $\alpha\text{-Al}_2\text{O}_3$ , thus less protective against oxidation, thus the appearance of the spinel  $\text{NiAl}_2\text{O}_4$  phase can be regarded that the specimen starts to lose good oxidation resistance. From this point, it is concluded that Pt-diffusion coatings have better oxidation resistance than Pt-Ir diffusion coatings developed by the electroplating method.

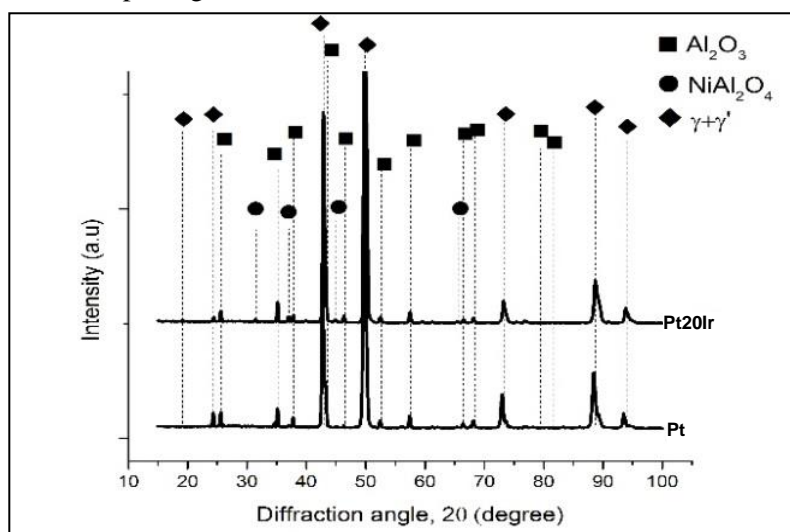


Figure 6. XRD patterns of specimens after 100 oxidation cycles.

Figure 7 shows the cross-sectional microstructure of the as-annealed coatings and coatings after 100 cyclic oxidation test at 1150 °C. When the specimens are exposed at high temperature, not just the microstructure of the coated layer, but also substrate are changed caused by the interdiffusion of elements between the coating layer and the substrate. Al diffused outwardly from the substrate to the surface to form the protective alumina. In this study, to protect the alumina scale on the surface of samples, a Cu layer was electroplated over all the sample before cross-sectional cutting and metallography preparation. With this method, the alumina scale on the surface of sample could be seen clearly as the black colour, dense and continuously. Meanwhile, Pt and Ir diffused inwardly to substrate, which gives rise to the growth of IDZ. The difference of diffusion rate of the elements results in the formation of voids due to Kirkendall effect [18]. The Kirkendall voids could degrade the mechanical property of the specimens. Although Pt electroplated specimen showed the better oxidation resistance with low mass change with the formation of dense and uniform  $\alpha\text{-Al}_2\text{O}_3$  scale on the surface, the cross-sectional microstructure revealed the rapid formation of voids in the substrate region beneath the IDZ. These voids could develop and connect each other, then drastically deteriorate the mechanical properties. On the other hand, the Pt20Ir diffusion coatings showed slower microstructure change with less and smaller voids in the substrate due to the lower diffusivity of Ir. The IDZ of Pt20Ir coating after 100 cycles of oxidation is also thinner than that of Pt electroplated specimen.

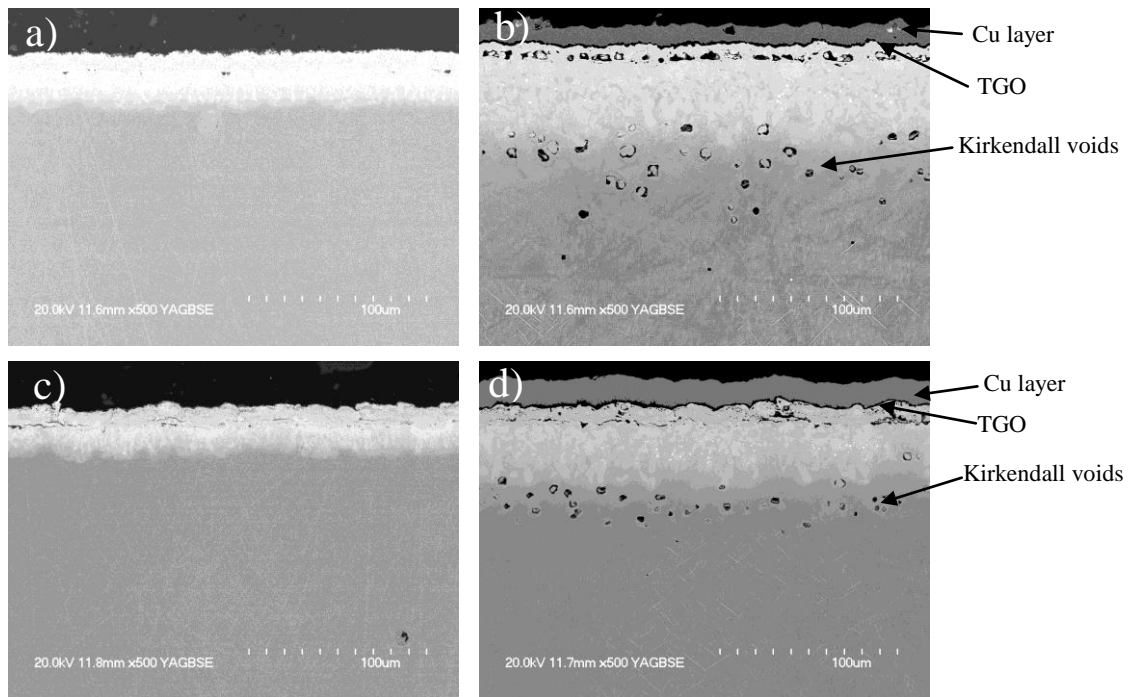


Figure 7. Cross-sectional microstructure of coatings after cycle test

- |                                |                               |
|--------------------------------|-------------------------------|
| a) Pt plating – As annealing   | b) Pt plating – 100 cycles    |
| c) PtIr plating – As annealing | d) PtIr plating – 100 cycles. |

During exposure at high temperature, elements on the surface reacted with oxygen to form an oxide scale called thermally grown oxide (TGO). Materials with good oxidation resistance should perform less amount of surface spallation, and once the spallation occurs, immediate reforming of the protective scale forms, which plays a main role for prolonging the life time of coatings.

To possess better oxidation resistance is one of the most important requirements of bond-coating for thermal barrier coating systems (TBC) on Ni base single crystal superalloys for gas turbines. When the coatings are exposed at high temperature environment, some elements on the surface will react with oxygen to form an oxide scale termed as a thermally grown oxide (TGO). Once TGOs grow to some extent, they tend to spall off from the surface due to the thermal strain caused by the difference in thermal expansion coefficients between the coating layer and TGOs. Even if the spallation occurs, immediate reforming of the protective TGO can maintain the oxidation resistance, which plays a main role for prolonging the life time of coatings. In this sense,  $\alpha$ - $\text{Al}_2\text{O}_3$  with stable and slower growth rate is regarded as the most protective TGO above 1000 °C. In this study, after 100 cycles of oxidation, surface of the Pt diffusion coating was covered with protective  $\alpha$ - $\text{Al}_2\text{O}_3$  layer, whereas spinel  $\text{NiAl}_2\text{O}_4$  was observed in the Pt-Ir coating as confirmed from Figs.4 and 6, revealing that the Pt diffusion coating developed by the electroplating method has better oxidation resistance. On the other hand, microstructural stability of the substrate is better in the PtIr coating. Then layer to protect coating and substrate from further oxidation. Since the life time of the component is controlled by both oxidation resistance and mechanical properties. Further development of coatings having



both good resistance with slower microstructure change is required, which may be an optimization of electroplating, or novel coating process. Such attempts are now underway.

#### 4. CONCLUSION

The Pt and Pt20Ir diffusion coating were fabricated successfully on the single crystal superalloy by electroplating method. The cyclic oxidation test was used to evaluate the effect of Ir addition to the microstructure change and oxidation behavior of coating. The results can be summarized as follows:

- Ir addition results in the cracking on the surface of electroplated layer.
- Uphill diffusion of Al to the surface was observed in both Pt and Pt20Ir coatings, which led to the formation of the protective scale. The Al concentration on the surface of Pt and Pt20Ir coating is 20 at.% and 18 at.%, respectively.
- Ir addition to the Pt-diffusion coatings affects the diffusion of elements and results in the formation of  $\alpha(\text{NiPt}_2\text{Al})$  phase by the annealing treatment. The  $\alpha(\text{NiPt}_2\text{Al})$  phase was transformed to  $\gamma'$  in the passage of oxidation tests.
- Ir addition to the Pt-diffusion coatings retarded the formation of voids in the coatings and substrate after 100 cyclic oxidation test.

**Acknowledgement.** Part of this work has been carried out under the IMS-NIMS international cooperative graduate program. The authors are also grateful for Mr. M. Murakami for conducting electrodeposition and Dr. A. Ishida for fruitful discussions.

#### REFERENCES

1. Darolia R. - Thermal barrier coatings technology: Critical review, progress update, remaining challenges and prospects, *Int. Mater. Rev.* **58** (6) (2013) 315-348.
2. Rajendran R. - Gas turbine coatings – An overview, *Engineering Failure Analysis* **26** (0) (2012) 355-369.
3. Tolpygo V. K. and Clarke D. R. - Surface rumpling of a (Ni, Pt)Al bond coat induced by cyclic oxidation, *Acta Mater.* **48** (13) (2000) 3283-3293.
4. Zhang Y., Stacy J. P., Pint B. A., Haynes J. A., Hazel B. T., Nagaraj B. A. - Interdiffusion behavior of Pt-diffused  $\gamma + \gamma'$  coatings on Ni-based superalloys, *Surf. Coat. Technol.* **203** (5-7) (2008) 417-421.
5. Selezneff S., Boidot M., Hugot J., Oquab D., Estournès C., Monceau D. - Thermal cycling behavior of EBPVD TBC systems deposited on doped Pt-rich  $\gamma - \gamma'$  bond coatings made by Spark Plasma Sintering (SPS), *Surf. Coat. Technol.* **206** (7) (2011) 1558-1565.
6. Tue D. C., Akitoshi W., Akio N., Hideyuki M., and Lien Le Thi Hong - Microstructure and high temperature oxidation resistance of Pt and Pt-Ir diffusion coatings on Ni base superalloy, *Vietnam Journal of Science and Technology* **53** (1B) (2015) 497-458 (in Vietnamese).
7. Izumi T., Wang X., Atkinson A. - Effects of targeted  $\gamma$ -Ni +  $\gamma'$  -Ni3Al-based coating compositions on oxidation behavior, *Surf. Coat. Technol.* **202** (4-7) (2007) 628-631.

8. Wu R. T., Wang X., and Atkinson A. - On the interfacial degradation mechanisms of thermal barrier coating systems: Effects of bond coat composition, *Acta Mater.* **58** (17) (2010) 5578-5585.
9. He D., Guan H., Sun X., Jiang X. - Manufacturing, structure and high temperature corrosion of palladium-modified aluminide coatings on nickel-base superalloy M38, *Thin Solid Films* **376** (1-2) (2000) 144-151.
10. Murakami H., Yano T., and Sodeoka S. - Process Dependence of Ir-Based Bond Coatings, *Materials Transactions.* **45** (9) (2004) 2886-2890.
11. Yamabe-Mitarai, Y. and Aoki H. - Solid-solution hardening of Ir by Pt and Ni. *Mater. Lett.* **56**(5) (2002) p. 781-786.
12. Wu F., Murakami H., and Suzuki A. - Development of an iridium-tantalum modified aluminide coating as a diffusion barrier on nickel-base single crystal superalloy TMS-75, *Surf. Coat. Technol.* **168** (1) (2003) 62-69.
13. Wu Y. N., Yamaguchi A., Murakami H., Kuroda S. - Hot corrosion behavior of Pt-Ir modified aluminide coatings on the nickel-base single crystal superalloy TMS-82+, *J. Mater. Res.* **22** (1) (2007) 206-216.
14. Suzuki A., Wu Y., Yamaguchi A., Murakami H., Rae C. M. F. - Oxidation behavior of Pt-Ir modified aluminized coatings on Ni-base single crystal superalloy TMS-82+, *Oxid. Met.* **68** (1-2) (2007) 53-64.
15. Hayashi S., Ford S. I., Young D. J., Sordelet D. J., Besser M. F., Gleeson B. -  $\alpha$ -NiPt(Al) and phase equilibria in the Ni-Al-Pt system at 1150 °C, *Acta Mater.* **53** (11) (2005) 3319-3328.
16. Stacy J. P., Zhang Y., Pint B. A., Haynes J. A., Hazel B. T., Nagaraj B. A. - Synthesis and oxidation performance of Al-enriched  $\gamma + \gamma'$  coatings on Ni-based superalloys via secondary aluminizing, *Surf. Coat. Technol.* **202** (4-7) (2007) 632-636.
17. Terock M., Fleischmann E., Hochmuth C., Völkl R., Glatzel U. - Synthesis and characterization of a Pt-Al-Cr-Ni  $\gamma/\gamma'$  -coating on the Ni-based superalloy CMSX - 4, *Surf. Coat. Technol.* **236** (2013) 347-352.
18. Audigié P., Rouaix-Vande Put A., Malié A., Bilhé P., Hamadi S., Monceau D. - Observation and modeling of  $\alpha$ -NiPtAl and Kirkendall void formations during interdiffusion of a Pt coating with a  $\gamma$ -(Ni-13Al) alloy at high temperature, *Surf. Coat. Technol.* **260** (2014) 9-16.